https://doi.org/10.5194/egusphere-2026-5425
Preprint. Discussion started: 14 September 2026

From sedimentary production to water-column accumulation: temperature and spatial controls on littoral methane

Katharina J. Kiefel[1], Frank Peeters[1], Armando Sepulveda-Jauregui[1,2,A], L. Loraine Ropella[3], Karla Martinez-Cruz[1]

[1]Limnological Institute, Department of Biology, University of Konstanz, Konstanz, 78464, Germany
[2]Department of Plankton and Microbial Ecology, Leibniz-Institute of Freshwater Ecology and Inland Fisheries IGB, Berlin, 12587, Germany
[3]Department of Marine Sciences, University of Gothenburg, Gothenburg, 405 30, Sweden
[A]Current address: Department of Microbial Ecology, The Federal Institute of Hydrology, Koblenz, 56068, Germany

Correspondence to: Karla Martinez-Cruz (karla.martinez@uni-konstanz.de)

Abstract. Littoral sediments are important sources of methane (CH_4) to lake water, but it remains unclear how strongly sedimentary CH_4 production controls sediment-water fluxes and dissolved CH_4 concentrations across seasons and spatially heterogeneous littoral zones. We measured sediment organic carbon, potential CH_4 production, sediment-water CH_4 fluxes, dissolved CH_4 concentrations, and stable carbon isotopes of CH_4 and CO_2 at seven littoral sites in Upper Lake Constance (ULC) and Lower Lake Constance (LLC) over four seasons. Potential CH_4 production, sediment-water CH_4 fluxes, and dissolved CH_4 concentrations were significantly related and showed similar temperature dependencies. Their apparent activation energies ranged from 0.81 to 1.11 eV and did not differ significantly. These results are consistent with a process chain from sedimentary production via sediment-water fluxes to dissolved CH_4, although the shared temperature dependence of the three variables means that their relationships do not, by themselves, demonstrate causal propagation along this chain. Spatial patterns, however, became weaker along this process chain. Within ULC, differences in potential CH_4 production were reflected in sediment-water fluxes but were no longer significant in dissolved CH_4 concentrations. Between the two lakes, dissolved CH_4 concentrations were significantly higher in LLC than in ULC, whereas potential CH_4 production and sediment-water CH_4 fluxes did not differ significantly. Potential CH_4 production increased with sediment organic carbon, suggesting that substrate availability may have contributed to spatial differences in CH_4 production. Carbon isotope patterns were consistent with a sedimentary, mainly acetoclastic CH_4 source and indicated modification of part of the dissolved CH_4 pool after release from the sediment. However, oxidation alone could not explain the isotopic contrast between the lakes, suggesting an additional influence of lateral mixing and hydrodynamic transport. Our results suggest that sedimentary CH_4 production contributes to controlling littoral CH_4 supply, whereas oxidation and physical transport can weaken or redistribute this signal in the water column.

https://doi.org/10.5194/egusphere-2026-5425
Preprint. Discussion started: 14 September 2026

1 Introduction

Inland waters play an important role in the global carbon cycle and contribute substantially to greenhouse gas emissions (Lauerwald et al., 2023). Although lakes cover only 2.2 % of the Earth's land surface, they emit approximately 53 Tg CH_4 yr^{-1} (Saunois et al., 2025). Large lakes (> 100 km^2) are an important but still understudied component of global CH_4 budgets (Bastviken & Johnson, 2025; Peacock et al., 2023; Saunois et al., 2025).

CH_4 is primarily formed in anoxic sediments through methanogenesis and reaches the water column through diffusion, ebullition, and plant-mediated transport (Bastviken, 2009; Bodmer et al., 2024). CH_4 can also be produced in oxygenated lake water, although the importance and underlying mechanisms of this source vary among lakes (Hilt et al., 2022). In large lakes, dissolved CH_4 concentrations are typically much higher in the littoral than in the pelagic zone because littoral waters are directly connected to CH_4-producing sediments, whereas the pelagic surface waters lack a comparable local sediment source (Khatun et al., 2024; Saunois et al., 2025). Within the littoral zone, however, CH_4 concentrations can vary strongly over short distances. This variability may reflect differences in sediment properties and sediment organic carbon (SOC) content, which influence CH_4 production, as well as differences in physical transport processes that transfer CH_4 from the sediment into the water column and redistribute it towards offshore areas (DelSontro et al., 2018). In shallow littoral areas, surface waves can further enhance CH_4 release by disturbing the sediment (Hofmann et al., 2010), whereas this process is largely absent in deeper pelagic areas.

Temperature provides another important source of variability because sedimentary CH_4 production increases strongly with temperature (Schulz et al., 1997; Duc et al., 2010; Lavergne et al., 2021). Shallow littoral sediments experience comparatively large seasonal changes in temperature, and warming may enhance their sedimentary CH_4 production (Bastviken et al., 2008; Sepulveda-Jauregui et al., 2018; Jansen et al., 2022). After entering the water column, part of the dissolved CH_4 is oxidised by methanotrophs, while the remainder may accumulate, be emitted to the atmosphere, or be transported towards the pelagic zone. Previous studies have shown that CH_4 produced in the littoral can account for a large fraction of whole-lake CH_4 emissions (Encinas Fernández et al., 2016; Peeters et al., 2019; Peeters & Hofmann, 2021), highlighting the importance of littoral processes for the lake-wide CH_4 release. However, most studies have been based on one or a few sampling sites or short sampling periods. This makes it difficult to separate seasonal variability from spatial differences and may bias estimates of the littoral contribution to whole-lake CH_4 emissions (Natchimuthu et al., 2016; Peacock et al., 2023). It also remains unclear whether the temperature dependence of sedimentary CH_4 production is reflected in sediment-water CH_4 fluxes and dissolved CH_4 concentrations when spatial differences among littoral sites are considered.

In this study, we investigated littoral CH_4 cycling in Upper and Lower Lake Constance (ULC and LLC, respectively). ULC is one of the largest lakes in Central Europe, with a surface area of 472 km^2 and a maximum depth of 251 m. LLC lies downstream of ULC and therefore experiences similar climatic conditions but differs strongly in size, morphology, water chemistry and hydrodynamics. Previous research has shown pronounced spatial and seasonal variability in dissolved CH_4 concentrations across ULC and LLC (Hofmann, 2013; Encinas Fernández et al., 2016). Several factors may contribute to this variability,

https://doi.org/10.5194/egusphere-2026-5425
Preprint. Discussion started: 14 September 2026

including SOC content, temperature, hydrodynamic mixing, oxygen availability, and macrophyte coverage (Bertolet et al., 2022; Bodmer et al., 2024; Kang et al., 2024). However, it remains unclear how spatial heterogeneity in sediment properties, lake morphology, hydrodynamics, and CH_4 oxidation modify the relationships between sedimentary CH_4 production, sediment-water CH_4 fluxes, and dissolved CH_4 concentrations.

Dissolved CH_4 concentrations reflect the balance between CH_4 inputs from the sediments, oxidation, atmospheric emission, and lateral transport. Here, we combined measurements of SOC content as an indicator of substrate availability, potential CH_4 production rates as an indicator of microbial production capacity, sediment-water CH_4 fluxes and dissolved CH_4 concentrations. We additionally analysed the stable carbon isotopic composition of CH_4 ($\delta^{13}C\text{-}CH_4$) and carbon dioxide ($\delta^{13}C\text{-}CO_2$) to infer dominant methanogenic pathways and assess the possible influence of CH_4 oxidation in surface sediments and the overlying water column. Measurements were conducted at seven littoral sites in ULC and LLC over different seasons and temperatures. This dataset allowed us to investigate the relationships between potential CH_4 production rates, sediment-water CH_4 fluxes, and dissolved CH_4 concentrations while accounting for temperature variability and spatial differences among sites. Based on this data, we tested the following hypotheses: (i) littoral dissolved CH_4 concentrations are primarily controlled by a bottom-up process chain in which higher potential CH_4 production rates result in larger sediment-water CH_4 fluxes, which in turn lead to higher dissolved CH_4 concentrations; (ii) potential CH_4 production rates increase with temperature, and this temperature dependence is reflected in sediment-water CH_4 fluxes and dissolved CH_4 concentrations; and (iii) spatial differences in sediment-water CH_4 fluxes and dissolved CH_4 concentrations reflect spatial differences in potential CH_4 production rates, which are related to differences in SOC content. By combining sediment properties, potential CH_4 production, sediment-water CH_4 fluxes, dissolved CH_4 concentrations, and stable carbon isotopes, this study examines how CH_4 production, transport, and oxidation jointly determine littoral CH_4 dynamics in two connected lakes of contrasting size and morphology.

2 Materials and Methods

2.1 Study Site and Sampling Strategy

Field sampling was carried out in 2024 in Upper and Lower Lake Constance (Fig. 1). ULC is a large, oligotrophic, monomictic lake with a surface area of 472 km^2 and a maximum depth of 251 m located in Central Europe and bordered by Germany, Switzerland, and Austria (IGKB, 2022). LLC is located downstream of ULC, has a surface area of 62 km^2 and a maximum depth of 45 m. We selected seven littoral sampling sites, four in ULC and three in LLC (Fig. 1). All three sites in LLC are located in Gnadensee (Fig. 1) which is the most enclosed sub-basin of LLC. Gnadensee is separated from the other basins of LLC by a narrow and shallow sill (average water depth of about 2.5 m) and has a surface area of approximately 13 km^2 and a maximum depth of 19 m (Wessels et al., 2015; IGKB, 2022). The main characteristics of each sampling site are listed in Table S1.

https://doi.org/10.5194/egusphere-2026-5425
Preprint. Discussion started: 14 September 2026

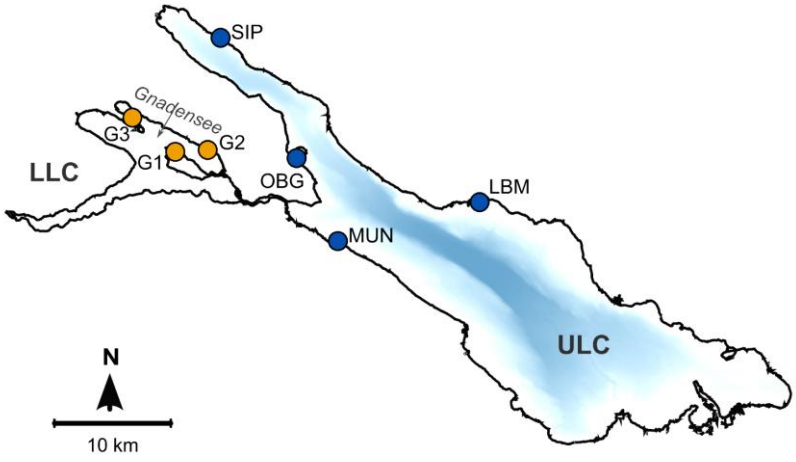

Figure 1: Map of Lake Constance with littoral sampling sites. Gold and blue circles indicate sampling sites in Lower Lake Constance (LLC) and Upper Lake Constance (ULC), respectively. Lake depth is represented by blue shading, with lighter tones indicating shallower areas and darker tones indicating deeper areas (maximum depth: 251 m).

Dissolved CH_4 concentrations were measured during seasonal campaigns over one year to capture spatial and seasonal variability among the study sites. During each campaign, we additionally collected (i) sediment samples for incubation experiments to determine potential CH_4 production, (ii) sediment cores to measure sediment-water CH_4 fluxes, and (iii) water and sediment samples for $\delta^{13}C$-CH_4 and $\delta^{13}C$-CO_2 analysis. Spring sampling was conducted in April and May for isotopes (see below) in ULC (mean water temperature ± standard deviation, 12 ± 3 °C) and in May in LLC (18 ± 2 °C), followed by summer sampling in July-August (24 ± 1 °C), autumn sampling in October-November (13 ± 1 °C), and winter sampling in December (7 ± 1 °C). Further details on sampling dates and water temperatures are provided in Table S1.

All sampling campaigns were conducted during dry and calm weather periods to minimise sediment disturbance and CH_4 outgassing. Hourly wind-speed data from the DWD weather station in Constance, Germany indicated that wind speed at the time of sampling was below 5 m s^{-1} during all campaigns (Deutscher Wetterdienst, 2024).

2.2 Dissolved CH_4 and Carbon Stable Isotopes $\delta^{13}C$-CH_4 and $\delta^{13}C$-CO_2 in Water Samples

During each sampling campaign, water samples for dissolved CH_4 and stable isotopes analyses ($\delta^{13}C$-CH_4 and $\delta^{13}C$-CO_2) were collected using a vertical Limno Sampler 2.0 L (Limnos, Poland). At each site, three replicate water samples were collected at approximately mid-depth (0.5–1 m), where the total water-column depth was approximately 1–2 m. Additional water samples for stable-isotope analyses were collected immediately above the sediment surface. Dissolved CH_4 in the water samples was measured using the headspace method, as previously described by Casper et al. (2003). Briefly, replicate water samples were taken from the sampler using 60 mL syringes and immediately injected into 120 mL serum bottles previously prepared with an oversaturated solution of sodium chloride (45 mL), sealed with a butyl rubber stopper (WICOM GmbH, Germany) and evacuated (- 0.9 ± 0.1 bar). The headspace gas was analysed within 48 h after the sampling campaign. For this purpose, the gas was injected into a custom-made discrete sample inlet port connected to the Ultra-Portable Greenhouse Gas Analyzer with

https://doi.org/10.5194/egusphere-2026-5425
Preprint. Discussion started: 14 September 2026

1 Hz resolution (UGGA-30p, Los Gatos Research, USA). We used a continuous stream with a flow rate of 0.5 L min^{-1} of ultra-high purity nitrogen (N_2 UHP, 99.999 Vol. %, Sauerstoffwerk Friedrichshafen GmbH, Germany) for a zero CH_4 baseline. The measuring system was calibrated using standard gas mixtures of 10 ppm, 100 ppm, 1000 ppm, and 10 000 ppm CH_4 (Air Liquide GmbH, Germany), with a nominal precision of ~ 2 ppb (1s) and a linear measurement range from 0.01 to 100 ppm for CH_4 (Los Gatos Research, 2015). For each injection, the CH_4 peak area was determined using baseline-corrected trapezoidal integration in Matlab Version R2022b (MathWorks Inc., USA).

For dissolved $\delta^{13}C$-CH_4 and $\delta^{13}C$-CO_2 in the water, we collected 30 – 40 mL of water using triplicate 60 mL syringes. Then, we created a headspace with N_2 UHP in the remaining volume of the syringes. The syringes were then vigorously shaken for a minute to reach the gas phase equilibrium. The gas sample from the headspace was then transferred into 12 mL pre-evacuated (- 0.9 ± 0.1 bar) Exetainers (Labco, UK), slightly over pressurizing the gas in the vials for complete filling.

2.3 Sediment-Water CH_4 Fluxes

Eight sediment cores were collected at each sampling site during each campaign using a gravity corer equipped with polycarbonate liners of 5.9 cm internal diameter. The cores were retrieved with overlying water, sealed immediately after collection, and transported to the shore for measurement. Sediment-water CH_4 fluxes were measured using the non-invasive gas-accumulation method described by Lessmann (2018). Briefly, the overlying water was carefully removed until a water layer of approximately 1 cm remained above the undisturbed sediment surface. The liner was then sealed with a rubber stopper and connected to an Ultra-Portable Greenhouse Gas Analyzer (UGGA-30p; Los Gatos Research, USA) in a closed-loop configuration. The CH_4 mixing ratio in the gas phase was recorded for 3 min at a frequency of 1 Hz. Each core was measured in triplicate, and the mean of the three measurements was used as the flux estimate for that core.

The rate of change in the CH_4 mixing ratio, $\frac{\partial \chi_{CH4}}{\partial t}$ (ppm s^{-1}), was determined by linear regression. This rate was converted to the rate of change in the amount of CH_4 using the ideal gas law:

$$\frac{\partial n_{CH4}}{\partial t} = \frac{P\,V_{tot}}{R\,T}\left(\frac{\partial \chi_{CH4}}{\partial t} \times 10^{-6}\right) \quad (1)$$

where P and T are the ambient pressure (Pa) and gas temperature (K) measured during each determination, V_{tot} is the total gas volume of the closed loop (m^3), R is the ideal gas constant (8.314 J mol^{-1} K^{-1}). V_{tot} included the headspace above the overlying water, the connecting tubing, and the internal volume of the gas analyser. Sediment-water CH_4 flux was then calculated as

$$F_{CH4} = \frac{1}{A}\frac{\partial n_{CH4}}{\partial t} \quad (2)$$

where A is the cross-sectional area of the sediment core (m^2). Fluxes were converted from mol m^{-2} s^{-1} to mmol m^{-2} d^{-1}. Across all replicate core measurements, the mean coefficient of determination of the linear regressions was $R^2 > 0.75$.

2.4 Processing of Sediment Samples

Immediately after measuring the sediment-water CH_4 fluxes, from randomly five sediment cores per site the top section (0-5 cm) was sliced off. The sediment slices of each core liner at the top were pooled, providing for each site an average sample of

https://doi.org/10.5194/egusphere-2026-5425
Preprint. Discussion started: 14 September 2026

sediment from 0-5 cm. Then, approximately 10 g of each pooled sediment sample were dried at 90 °C for 48 hours. After the dry weight was measured, dried sediments were ground to fine powder and stored until further analysis of carbon content. SOC content was measured using an Elemental Analyser coupled to a Solid Sample Combustion Unit (TOC-Shimadzu, SSM-5000A, Shimadzu, Japan). The remaining sediment of each pooled sediment sample was stored at 3 °C in dark and used later for incubation experiments (see below).

The remaining three sediment cores per site were used to determine dissolved pore-water $\delta^{13}C\text{-}CH_4$ and $\delta^{13}C\text{-}CO_2$ from the top 5 cm and the bottom layers (5-20 cm). For this, 5 mL of wet sediment were gently transferred with a cut-off syringe into 120 mL serum vials containing 5 mL of CH_4- and CO_2-free distilled water. The vials were sealed with aluminium crimp caps (WICOM GmbH, Germany) and grey butyl rubber stoppers. Headspace equilibration was performed following the same procedure used for the isotope measurements in the water samples described above, except that the vials were shaken for 1 minute to equilibrate CH_4 and CO_2 with the headspace and the slurry. Subsequently, 15 mL of headspace from each sample were transferred into 12 mL pre-evacuated Exetainers.

To determine the relationship between sediment dry mass and sediment volume, subsamples of a known volume of homogenised sediment from each site were dried to constant weight at 90 °C and subsequently weighed. The resulting site-specific dry-mass-to-sediment-volume ratio was used to convert potential CH_4 production rates per sediment dry mass to rates per sediment volume (see below).

2.4.1 Sediment Incubations

To estimate the potential CH_4 production of each site, slurry incubation experiments were carried out using sediment samples retrieved during spring. The upper 5 cm of the sediment were used for the incubations since previous measurements in littoral sediments of Lake Constance showed maximum potential CH_4 production rates at 2–5 cm sediment depth (Thebrath et al., 1993). For each pooled sediment sample, we prepared one slurry containing sediment and sterile anoxic CH_4-free distilled water in a 1:1 v/v ratio. The slurry was divided into three subsamples providing triplicate incubation samples for each site. For each of the triplicate incubation samples, 30 mL of the slurry was transferred into 50 mL crimp vials under constant flushing with N_2 UHP. Flushing was maintained for five minutes until vials were sealed with butyl rubber stoppers and aluminium crimp caps. Because our incubations were conducted under anoxic conditions, the measured rates represent the potential methanogenic capacity of the surface sediment rather than in situ CH_4 production.

All vials were pre-incubated for three days at 28 °C to ensure the onset of methanogenesis inside the vials. After pre-incubation, all samples were flushed for five minutes with N_2 UHP. The vials were then kept at either 3 °C, 10 °C or 20 °C for 30 – 120 d depending on CH_4 accumulation over time. The incubation temperatures were chosen to cover much of the range of sediment temperature during the sampling campaigns. The CH_4 concentration in the headspace of each vial was determined every 2 – 3 days (samples at 20 °C), or 4 – 5 days (samples at 3 °C and 10 °C), by collecting 0.5 mL of the headspace in the vials and measuring the CH_4 fraction in this gas using the UGGA 30p as described above. The total amount of CH_4 was calculated as the sum of the CH_4 in the headspace, obtained from the measured CH_4 concentration in the gas phase and the volume of the

https://doi.org/10.5194/egusphere-2026-5425
Preprint. Discussion started: 14 September 2026

headspace, plus the amount of dissolved CH_4 in the aqueous phase. The latter was calculated according to Henry's law using the temperature-dependent CH_4-solubility parametrisation of Wiesenburg and Guinasso (1979) and the volume of the aqueous phase. At the end of the incubations, the sediment in each vial was dried at 90 °C to constant weight to determine its dry mass. Determining dry mass separately for each vial accounted for differences in slurry dilution among replicates. Potential CH_4 production was determined from the linear increase in total CH_4 over time ($R^2 > 0.7$, more than six measurements). Rates were first normalized to the sediment dry mass in the respective vial and subsequently converted to rates per sediment volume using the site-specific dry-mass-to-sediment-volume ratio described above.

2.5 Stable Isotopes $\delta^{13}C$-CH_4 and $\delta^{13}C$-CO_2 from Water and Sediment Measurements

We measured $\delta^{13}C$-CH_4 and $\delta^{13}C$-CO_2 in samples retrieved from the water column and pore water from sediment samples using an infrared Cavity Ring-Down Spectrometer (CRDS, Picarro G2201, Picarro Inc., USA) coupled with a Small Sample Isotope Module (SSIM), with Vienna Pee Dee Belenmite-VDPB (precision ± 0.55 ‰ $\delta^{13}C$-VPDB for CH_4 and CO_2) as reference. Briefly, from each sample collected in Exetainers as described above, 5 mL of gas sample were extracted and injected into the SSIM system.

For the analysis of isotopic signatures of CH_4, the results of isotopic measurements were sorted according to the range of CH_4 concentrations. High Range (HR) results were used when the CH_4 concentration was between 25 and 1000 ppm according to the findings of Brandily et al. (2021). High Precision (HP) results were used for methane concentrations below 25 ppm. $\delta^{13}C$-CO_2 values were corrected and calibrated following an empirical approach (see Supplementary Information, Fig. S1).

2.6 Data Analysis

Statistical analyses were conducted to assess seasonal, spatial, and process-related variability in CH_4 cycling across sites and lakes. Potential CH_4 production, sediment-water CH_4 fluxes, and dissolved CH_4 concentrations were log-transformed prior to further analysis. Replicate measurements were averaged to provide mean and standard error of the log-transformed properties for each station at each sampling time. When displayed in bar plots, the properties were transformed back to allow depiction in common units. All analyses were performed in MATLAB (version R2022b; MathWorks, Natick, MA, USA).

2.6.1. Descriptive Comparisons of Seasonal and Temperature Effects

The averaged log-transformed dissolved CH_4 concentrations and sediment-water CH_4 fluxes from the different stations were compared across seasons using Welch's one-way ANOVA allowing for unequal variances among seasons. When a significant overall seasonal effect was detected, pairwise Welch's t-tests with Holm correction for multiple comparisons were used as post-hoc tests to identify differences between seasons. Analyses were conducted separately for different levels of aggregation, i.e. considering all stations combined, distinguishing between the two lakes, and for each of the individual stations.

https://doi.org/10.5194/egusphere-2026-5425
Preprint. Discussion started: 14 September 2026

Temperature dependence of potential CH_4 production (P_{CH4}) was analysed using an Arrhenius equation assuming that the activation energy (E_a) for CH_4 production is independent of site:

$$P_{CH4,si}(T) = P_{CH4,si}(T_{ref}) \cdot e^{-\frac{E_a}{k_b}\left(\frac{1}{T}-\frac{1}{T_{ref}}\right)} \quad (3)$$

where $P_{CH4,si}(T)$ is the potential CH_4 production at site *si* and temperature T, $P_{CH4,si}(T_{ref})$ is the potential CH_4 production at the reference temperature T_{ref} (20 °C), E_a is the activation energy, and k_B the Boltzmann constant ($k_B = 8.62 \cdot 10^{-5}$ eV K^{-1}). Note that we allow a different $P_{CH4,si}(T_{ref})$ for each site. The coefficients of the Arrhenius relationship were obtained by multiple linear regression of the log-transformed Arrhenius equation using the model:

$$\log\left(P_{CH4}(T)\right) = \sum_{si=1}^{7}(S_{si} \cdot \alpha_{si}) - \beta \cdot \left(\frac{1}{T} - \frac{1}{T_{ref}}\right) \quad (4)$$

where $log(P_{CH4}(T))$ represents a vector of all measurements of $P_{CH4,si}$, each S_{si} is a vector for the respective station *si* containing 1 for all measurements from this station and zero for all others, and $\left(\frac{1}{T} - \frac{1}{T_{ref}}\right)$ is a vector of the temperature-dependence term in the Arrhenius equation based on all measurements of T corresponding to the measurements of potential CH_4 production. Treating all S_{si} and the temperature term as predictor variables and $log(P_{CH4}(T))$ as response variable, multiple linear regression can be used to estimate intercepts α_{si} and the common slope β. The parameter α_{si} corresponds to $log(P_{CH4,si}(20\ °C))$ and $\beta = E_a/k_b$. The multiple linear regression approach (Eq. (4)) is analogous to a linear model with a categorical variable representing sampling site but has the advantage that the fitted values of α_{si} and their standard errors can be directly interpreted as the values and standard errors of P_{CH4} at 20 °C at the different sites *si*.

Based on the results obtained from Eq. (4), we predicted values of $log(P_{CH4})$ for the temperatures and the sites at which the sediment-water CH_4 fluxes were measured, because incubation temperatures did not exactly match in situ sediment temperatures.

The same Arrhenius framework as in Eq. (4) was applied to sediment-water CH_4 fluxes and dissolved CH_4 concentrations, using sediment temperature and water temperature, respectively. In all cases, the models were fitted with site-specific intercepts and a common slope E_a/k_b describing the temperature dependence.

To test whether temperature sensitivities differed among potential CH_4 production, sediment-water CH_4 flux, and dissolved CH_4 concentrations, we fitted a combined linear model of the form $log(Y) \sim Process \times (1/T) + Process \times Site$. Here, Y represents the measured response variable and *Process* is a categorical variable with three levels: potential CH_4 production, sediment-water CH_4 fluxes, or dissolved CH_4. *Site* accounted for site-specific differences within each process. The Process × (1/T) interaction tested whether the Arrhenius slopes differed among processes. Three pairwise comparisons were performed (potential CH_4 production vs. sediment-water CH_4 flux, potential CH_4 production vs. dissolved CH_4, and sediment-water CH_4 flux vs. dissolved CH_4), and the resulting p-values were adjusted for multiple comparisons using the Holm correction.

https://doi.org/10.5194/egusphere-2026-5425
Preprint. Discussion started: 14 September 2026

2.6.2 Cross-process Relationships

To test whether sediment-water CH_4 fluxes are linked to potential CH_4 production rates and dissolved CH_4 to sediment-water CH_4 fluxes, we applied a linear regression approach on log-transformed variables. Specifically, we analysed relationships between (i) log-transformed sediment-water CH_4 fluxes and potential CH_4 production predicted at corresponding sediment temperatures and converted from dry-weight-based to volumetric units, as described above, and (ii) log-transformed dissolved CH_4 and sediment-water CH_4 fluxes. Because all properties had substantial uncertainty, we utilised weighted Deming regression considering independent errors of the respective properties along x- and y-axes for each observation. Model performance was evaluated using an F-test derived from an R^2-type metric (extending the R^2 g approach by Bossé et al., 2023). Parameter uncertainty was estimated using a leave-one-out jackknife procedure. Standard errors, 95% confidence intervals, and p values for testing whether the slope differed from zero or one were derived from the jackknife estimates.

2.6.3 Spatial Differences of Process Rates and Dissolved CH_4

Spatial differences of potential CH_4 production rates, sediment-water CH_4 fluxes, and dissolved CH_4 concentrations were evaluated at reference temperature 20 °C. Log-transformed values of potential CH_4 production rates, sediment-water CH_4 fluxes, and dissolved CH_4 at 20 °C were obtained from the Arrhenius framework (Eq. (4)) and correspond to the site-specific intercepts α_{si} fitted to the respective property. Pairwise differences among sites were assessed by testing linear contrasts between these fitted site-specific values. Standard errors of contrasts were calculated from the full covariance matrix of the fitted regression coefficients, thereby accounting for covariance among parameter estimates. For each response variable separately, the p-values of the 21 pairwise site comparisons were adjusted using the Holm correction.

We tested whether potential CH_4 production, sediment-water CH_4 fluxes, and dissolved CH_4 concentrations differed between ULC and LLC using separate random-effects models based on the site-specific estimates at 20 °C obtained from the corresponding Arrhenius models. For each property, the standard error of the difference between basin averages was estimated by combining the covariance matrix of the site-specific estimates from the Arrhenius model with the variability among sites estimated using restricted maximum likelihood. The significance of the difference between basin averages was evaluated using a two-sided t-test.

To explore potential drivers of spatial variability in potential CH_4 production rates, we related potential CH_4 production rates at 20 °C to sediment organic carbon (SOC). SOC values were log-transformed and averaged at the site level. The relationship between log (SOC) and log (CH_4 production rates) at 20 °C was evaluated using weighted Deming regression, accounting for uncertainty in both variables.

2.6.4 Stable Isotope Data Analysis

Spatial and seasonal variability in the $\delta^{13}C$-CH_4 was assessed after excluding spring because sampling in ULC and LLC occurred at different times and temperatures. Water-column and sediment samples were analysed separately to distinguish

https://doi.org/10.5194/egusphere-2026-5425
Preprint. Discussion started: 14 September 2026

between sedimentary source signatures and potential modification during transport through the water column. For water-column isotope samples, replicate measurements were first averaged within each sampling position. Because isotope values from mid-depth and immediately above the sediment were similar, values from the two positions were subsequently averaged within each site and season. The resulting site-level means were used as independent observations in all water-column isotope analyses. Site and seasonal effects in the water column were therefore evaluated using an additive linear model of the form $\delta^{13}C\text{-}CH_4 \sim Site + Season$. A Site × Season interaction was not included because only one independent water-column value was available for each site and season. Pairwise differences among sites and seasons were assessed using Tukey–Kramer post hoc comparisons.

Sediment analyses were restricted to the surface layer (0–5 cm), which is most directly connected to CH_4 transport across the sediment-water interface. The three independently collected sediment cores at each site and season were retained as biological replicates. Site-specific variability in surface-sediment $\delta^{13}C\text{-}CH_4$ was evaluated using a linear model of the form $\delta^{13}C\text{-}CH_4 \sim Site \times Season$. The significance of main effects and the interaction was evaluated by analysis of variance (ANOVA). Because the Site × Season interaction was significant, differences among sites within individual seasons were assessed using separate one-way ANOVAs followed by Tukey–Kramer post hoc comparisons.

Lake-scale differences were assessed separately within summer, autumn, and winter. For water-column isotope samples, the site-level means described above were used as independent observations. For surface sediments, the three independent cores were first averaged within each site and season so that sites, rather than individual cores, represented the independent replicates for each lake. Differences between ULC and LLC were evaluated using one-way ANOVA within each season, and the resulting three p-values were adjusted using the Holm procedure. Model assumptions were assessed by visual inspection of residual probability plots and plots of residuals against fitted values, which indicated no major deviations from normality or homoscedasticity.

3 Results

3.1 Seasonal and Spatial Variability in Littoral CH_4 Cycling

Spring measurements were excluded from the statistical comparison among seasons because sampling was conducted at different times and temperatures in ULC and LLC. Across summer, autumn, and winter, dissolved CH_4 concentrations differed significantly among seasons across all sites (Welch's ANOVA, $p < 0.001$) and when ULC and LLC were analysed separately (ULC: $p < 0.001$; LLC: $p = 0.002$). Holm-adjusted pairwise Welch's t-tests showed that dissolved CH_4 concentrations in ULC decreased significantly from summer to autumn and from autumn to winter. In LLC, concentrations were significantly higher in summer than in winter, whereas summer and autumn and autumn and winter did not differ significantly (Tables S6a – S6b). Sediment-water CH_4 fluxes also differed significantly among summer, autumn, and winter across all sites (Welch's ANOVA, $p < 0.001$) and within both ULC and LLC (both $p < 0.001$). In both lakes, fluxes were significantly higher in summer than in

https://doi.org/10.5194/egusphere-2026-5425
Preprint. Discussion started: 14 September 2026

autumn and winter, whereas autumn and winter did not differ significantly (Holm-adjusted post hoc tests, $p > 0.05$) (Tables S6a – S6b). This pattern was observed across all sites and when ULC and LLC were analysed separately.

Although spring was excluded from these statistical comparisons, spring dissolved CH_4 concentrations in ULC were broadly similar to those measured in autumn, consistent with the similar temperatures during the two campaigns (8–15 °C in spring and 12–13 °C in autumn). In LLC, spring concentrations were generally higher than in autumn but lower than in summer, corresponding to intermediate water temperatures in spring (16–19 °C), compared with autumn (14–15 °C) and summer (24–26 °C). This pattern suggests that the contrasting spring concentrations in ULC and LLC were related to differences in sampling temperature rather than to season alone (Table S1).

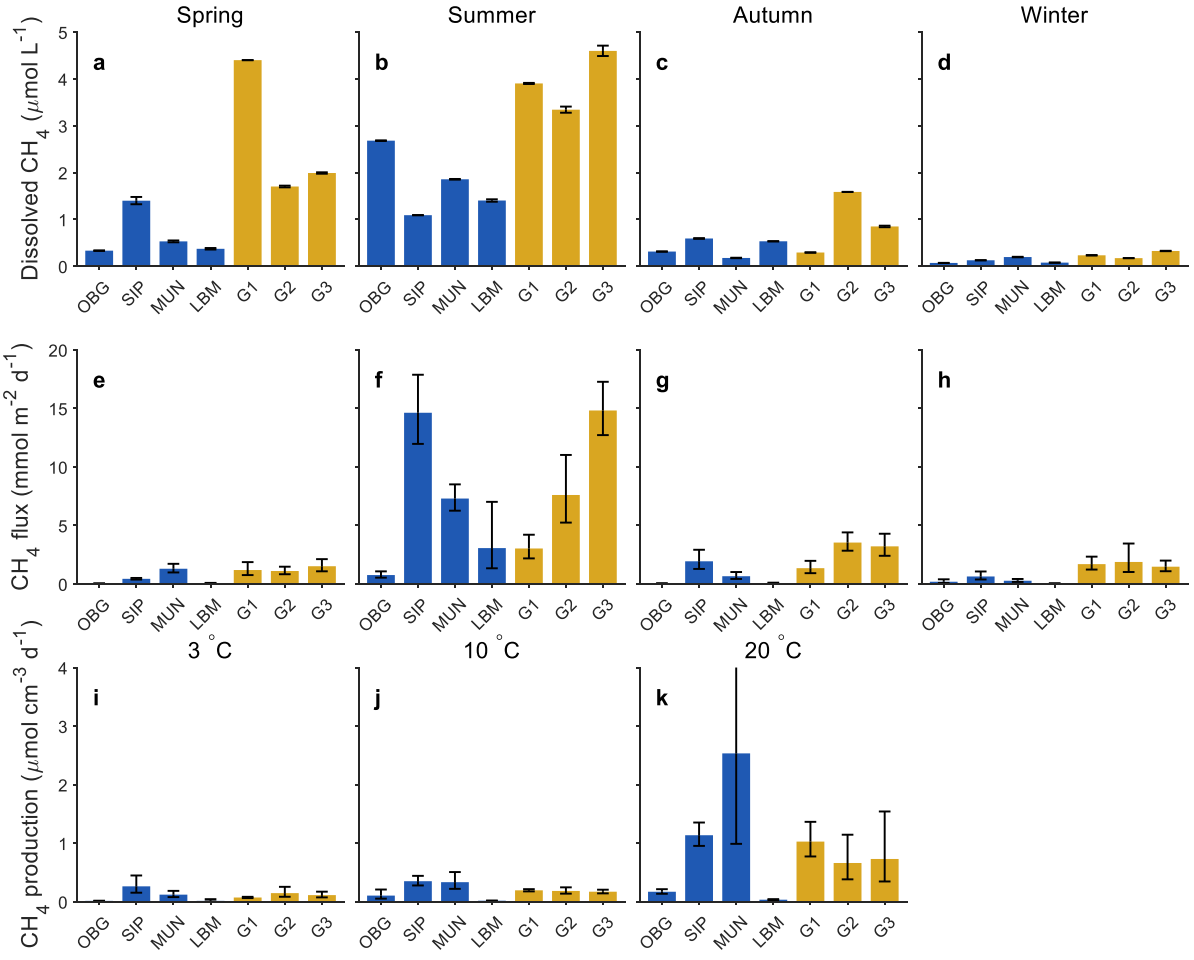

Figure 2: Seasonal dynamics of dissolved CH_4 and sediment-water CH_4 fluxes, the temperature dependence of potential CH_4 production and their spatial variability. Bar graphs of dissolved CH_4 (a-d) and sediment-water CH_4 fluxes (e-h) show geometric means of dissolved CH4 replicates (3 per site) and of sediment-water CH_4 fluxes (8 per site), respectively. Error bars indicate variability of the log-transformed data (± SE) and are therefore asymmetric on the linear scale. Bar graphs of potential CH_4 production (i-k) show the results from

https://doi.org/10.5194/egusphere-2026-5425
Preprint. Discussion started: 14 September 2026

the incubation experiments. ULC sites are depicted in blue, LLC sites in yellow. Sampling dates and the corresponding water and sediment temperatures at each site are provided in Table S1.

The temperature dependence of potential CH_4 production was well described by the Arrhenius model (Eq. 4), which explained 93% of the variance in log-transformed production rates ($R^2 = 0.93$, $p < 0.001$; Fig. S2). The model yielded an activation energy of $E_a = 0.81$ eV (SE = 0.10 eV, 95% CI: 0.56–1.03 eV; Fig. S3). Application of the same Arrhenius modelling approach to sediment-water CH_4 fluxes and dissolved CH_4 concentrations explained 53% and 80% of the variance, respectively (R^2 = 0.53 and 0.80, respectively; both $p < 0.001$; Fig. S2). The corresponding activation energies were $E_a = 0.94$ eV for sediment-water CH_4 fluxes (SE = 0.11 eV, 95% CI: 0.73–1.16 eV) and $E_a = 1.11$ eV for dissolved CH_4 concentrations (SE = 0.07 eV, 95% CI: 0.97–1.25 eV; Fig. S3; Table S4).

Pairwise comparisons of Arrhenius relationships across processes showed no significant differences between potential CH_4 production, sediment-water CH_4 fluxes, and dissolved CH_4 concentrations when accounting for site-specific differences (Holm-adjusted $p \geq 0.103$) (Tables S4a – S4b).

3.2 Links Among CH_4 Cycling Processes

The hypothesised links between sedimentary methanogenesis, sediment-water CH_4 fluxes, and dissolved CH_4 in littoral water were evaluated using weighted Deming regressions (Fig. 3).

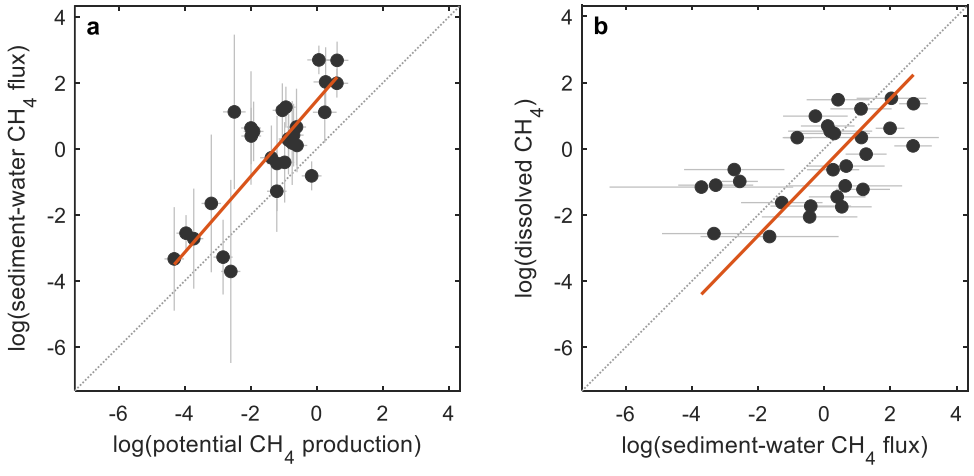

Figure 3: Linkage between potential CH_4 production, sediment-water CH_4 fluxes and dissolved CH_4. Weighted Deming regression accounting for uncertainties in both variables was applied to **(a)** log(sediment-water CH_4 fluxes) vs. log(potential CH_4 production) and **(b)** log(dissolved CH_4) vs. log(sediment-water CH_4 fluxes). Potential CH_4 production was predicted at in situ sediment temperatures using the Arrhenius model (Eq. (4)). Points represent site-specific means, with error bars indicating standard errors of log-transformed values. The red line indicates the best-fit regression, and the dotted line represents a slope of 1.

https://doi.org/10.5194/egusphere-2026-5425
Preprint. Discussion started: 14 September 2026

Log-transformed sediment-water CH_4 fluxes increased significantly with log-transformed potential CH_4 production rates (slope = 1.14, $p < 0.001$), and the slope was not significantly different from 1 ($p = 0.455$). Likewise, log-transformed dissolved CH_4 increased significantly with log-transformed sediment-water CH_4 fluxes (slope = 1.04; $p = 0.021$), and the slope did not differ significantly from 1 ($p = 0.933$; Table S5).

Together, these relationships are consistent with the hypothesised process chain linking potential CH_4 production rates in the sediment, sediment-water CH_4 fluxes and dissolved CH_4 accumulation in the littoral water.

3.3 Spatial Differences Along the CH_4 Process Chain

The Arrhenius model (Eq. (4)) applied to potential CH_4 production rates, sediment-water CH_4 fluxes, and dissolved CH_4 concentrations provided not only E_a but also coefficients α_{si}, which represent the log-transformed values of potential CH_4 production rates, sediment-water CH_4 fluxes, and dissolved CH_4 concentrations for each site at the reference temperature of 20 °C (Fig. 4).

In ULC, spatial differences among sites at the common reference temperature became less pronounced along the pathway from potential CH_4 production rates and sediment-water CH_4 fluxes to dissolved CH_4 (Fig. 4 b-d). Specifically, log-transformed potential CH_4 production rates were significantly higher at SIP and MUN than at OBG and LBM (adjusted $p \leq 0.002$). Log-transformed sediment-water CH_4 fluxes showed the same spatial pattern, with significantly higher fluxes at SIP and MUN than at OBG and LBM (adjusted $p < 0.001$). By contrast, differences in log-transformed dissolved CH_4 concentrations among ULC sites were less pronounced and not significant (adjusted $p \geq 0.932$).

In contrast to ULC, log-transformed potential CH_4 production rates, sediment-water CH_4 fluxes, and dissolved CH_4 concentrations did not differ significantly among G1, G2, and G3 in LLC (adjusted $p \geq 0.744$), indicating relatively homogeneous conditions within this lake (Table S9a).

At 20 °C, model-estimated dissolved CH_4 concentrations were significantly higher in LLC than in ULC ($p = 0.004$; Fig. 4d), whereas potential CH_4 production rates ($p = 0.515$; Fig. 4b) and sediment-water CH_4 fluxes ($p = 0.139$; Fig. 4c) did not differ significantly between lakes (Table S9b).

https://doi.org/10.5194/egusphere-2026-5425
Preprint. Discussion started: 14 September 2026

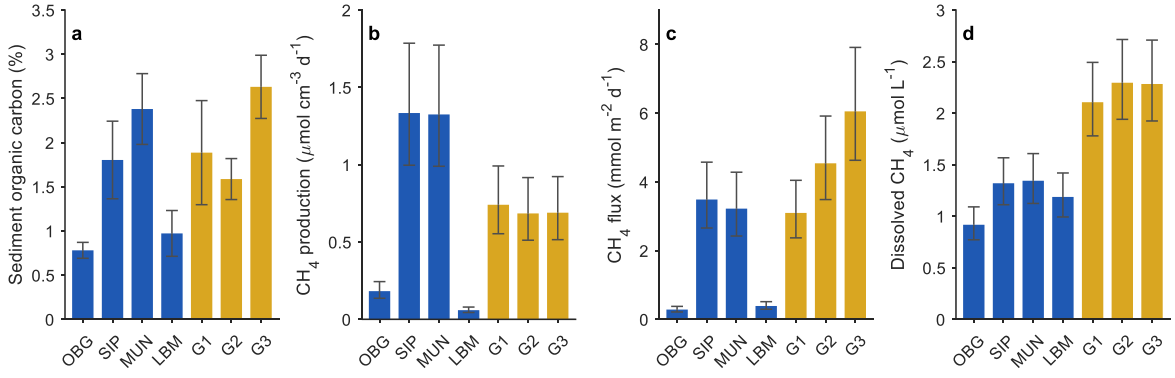

Figure 4: Spatial differences in sediment organic carbon (SOC) and CH_4 cycling variables across littoral sites. Panel (a) shows site-specific SOC values, whereas panels (b–d) show predicted values at the reference temperature of 20 °C for (b) potential CH_4 production, (c) sediment-water CH_4 fluxes, and (d) dissolved CH_4 concentrations. Predicted values and associated uncertainties were derived from the site-specific intercept coefficients (α_{si}) of the Arrhenius-type multiple linear regression model (Eq. (4)). Sites from ULC are shown in blue and sites from LLC in yellow.

Weighted Deming regression yielded a positive relationship between log-transformed SOC and potential CH_4 production at 20 °C, although the estimated slope was not significantly different from zero (slope = 1.19, p = 0.118; Fig. 5 and Table S5). Thus, sites with higher SOC tended to have higher potential CH_4 production, but the statistical evidence for this relationship was inconclusive.

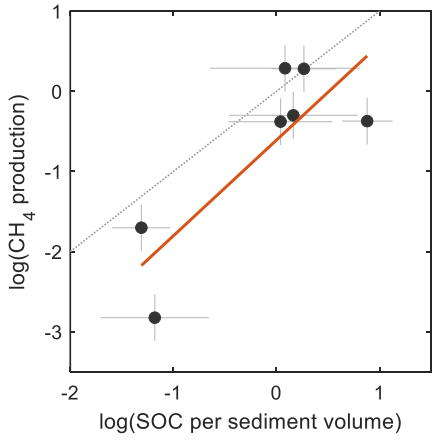

Figure 5: Linkage between potential CH_4 production and sediment organic carbon. Weighted Deming regression accounting for uncertainties in both variables was applied to log (CH_4 production) vs. log (SOC). Points represent site-specific means, with error bars indicating standard errors of log-transformed values. The red line indicates the best-fit regression, and the dotted line represents a slope of 1.

https://doi.org/10.5194/egusphere-2026-5425
Preprint. Discussion started: 14 September 2026

3.4 Stable Carbon Isotopes δ^{13}C-CH_4 and δ^{13}C-CO_2 from Water and Sediment

The relationship between δ^{13}C-CH_4 and δ^{13}C-CO_2 in water-column and sediment samples is shown in Fig. 6. Water-column δ^{13}C-CH_4 ranged from -58.70 ‰ to -28.35 ‰, whereas sediment δ^{13}C-CH_4 ranged from -65.05 ‰ to -42.70 ‰ (Fig. 6a, b). Thus, some water-column samples were more enriched in ^{13}C than the sediment samples, consistent with isotopic fractionation associated with CH_4 oxidation. The apparent fractionation factor (α_{app}), derived from δ^{13}C-CO_2 and δ^{13}C-CH_4 ranged from 1.025 – 1.085 in water-column samples and from 1.034 –1.075 in sediment samples. However, α_{app} did not differ significantly between paired water-column and sediment samples (paired t-test, p = 0.136) (Tables S2, S3, and S7).

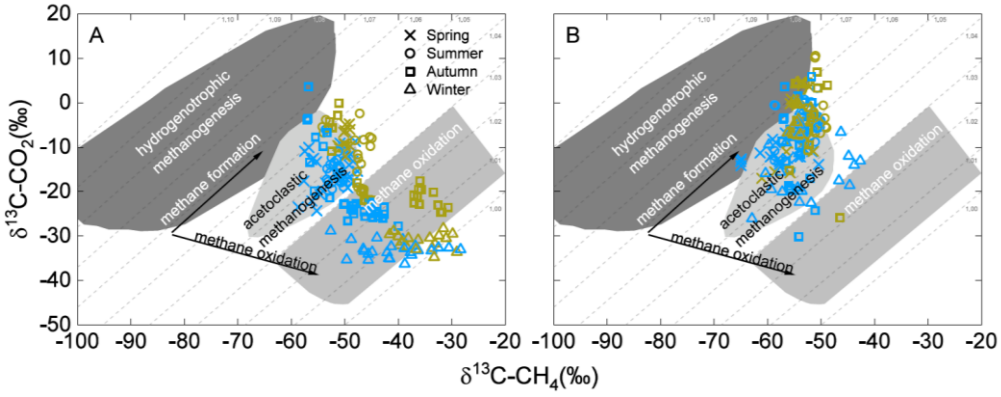

Figure 6: Stable carbon isotope composition and apparent fractionation. Measured stable carbon isotopic signatures of (a) water and (b) sediment samples. Sites from ULC are indicated in blue, sites from LLC are indicated in yellow. Grey isolines show the values of different α_{app}. Seasons are indicated with symbols (see legend). The hulls illustrate the observed δ^{13}C-CH_4 and δ^{13}C-CO_2 fractionation pathways of CH_4 processes according to Whiticar (1999).

Despite the substantial overlap of the sample distributions in isotope fractionation space, δ^{13}C-CH_4 varied significantly among sites and seasons in both sediments and the water column. In the water column, significant overall effects of site (p = 0.028) and season (p = 0.004) were detected, although none of the individual pairwise site comparisons were significant after Tukey–Kramer correction. In surface sediments (0 – 5 cm), δ^{13}C-CH_4 showed a significant site × season interaction (p < 0.001), indicating that spatial differences varied among seasons. At the lake scale, sedimentary δ^{13}C-CH_4 did not differ significantly between ULC and LLC within any individual season (p ≥ 0.231; Table S8d). In contrast, water-column δ^{13}C-CH_4 was consistently more depleted in ULC than in LLC, with significant differences in summer, autumn, and winter (adjusted p = 0.031, 0.046, and 0.046, respectively) (Tables S7a – S8d).

Site-specific differences in sedimentary δ^{13}C-CH_4 showed distinct and season-dependent spatial patterns. In summer, OBG was significantly more depleted than all other sites. In autumn, differences were generally weak, with a significant contrast detected only between SIP and G1. In winter, LBM was significantly more enriched than OBG, SIP, MUN, and all three LLC sites, while SIP was more depleted than several other sites. In contrast, sites within LLC (G1, G2, and G3) showed largely

https://doi.org/10.5194/egusphere-2026-5425
Preprint. Discussion started: 14 September 2026

similar isotopic signatures, with no significant differences among them in any season. Thus, site-specific variability was mainly associated with changing spatial patterns within ULC, whereas LLC remained comparatively homogeneous. Overall, water-column $\delta^{13}C\text{-}CH_4$ was consistently more depleted in ULC than in LLC, whereas sedimentary $\delta^{13}C\text{-}CH_4$ did not differ significantly between the two lakes.

4 Discussion

Our measurements revealed strong but distinct temperature and spatial patterns along the littoral CH_4 process chain. Potential CH_4 production, sediment-water CH_4 fluxes, and dissolved CH_4 concentrations all increased with temperature, whereas their site-level spatial patterns became less pronounced from sedimentary production and fluxes to dissolved CH_4. When the sampled sites were grouped by lake, only dissolved CH_4 concentrations differed significantly between ULC and LLC. In the following sections, we discuss the isotopic evidence for CH_4 production and transformation, the links among sedimentary CH_4 production, sediment-water fluxes, and dissolved CH_4 concentrations, and the processes that may explain their temperature dependence and spatial variation.

4.1 Isotopic Composition and Pathways of CH_4 Production and Transformation

The observed CH_4 isotopic signatures in the littoral zones of ULC and LLC were consistent with previously reported fractionation patterns for acetoclastic methanogenesis (Whiticar et al., 1986; Conrad, 2005; Londry et al., 2008). Acetate has also been identified as the dominant methanogenic substrate in both littoral (Thebrath et al., 1993) and profundal sediments of Lake Constance (Schulz et al., 1997). The overlap between sediment and water-column $\delta^{13}C\text{-}CH_4$ values was consistent with a sedimentary origin of dissolved CH_4. The comparatively enriched $\delta^{13}C\text{-}CH_4$ values in some water-column samples also suggested that CH_4 oxidation affected part of the dissolved CH_4 pool, with the clearest signal occurring during winter in both lakes.

Surface-sediment $\delta^{13}C\text{-}CH_4$ did not differ consistently between ULC and LLC, whereas water-column CH_4 was generally more depleted in ^{13}C in ULC than in LLC. Because oxidation preferentially consumes $^{12}CH_4$ and leaves the remaining CH_4 enriched in ^{13}C (Coleman et al., 1981; Whiticar, 1999), greater oxidation in LLC could explain its more positive water-column $\delta^{13}C\text{-}CH_4$ values. However, other processes could produce or contribute to this difference. For example, partial dissolution of isotopically depleted CH_4 bubbles could introduce sediment-derived CH_4 into the water column (Thebrath et al., 1993; McGinnis et al., 2006). Consequently, differences in ebullition or bubble dissolution between the lakes could contribute to their contrasting water-column isotopic signatures. Mixing with water containing CH_4 of a different isotopic composition may also have contributed to the observed contrast. Because the measured water-column isotope signatures integrate source composition, oxidation, bubble dissolution, and physical mixing, the relative contributions of these processes cannot be determined from the isotope data alone.

https://doi.org/10.5194/egusphere-2026-5425
Preprint. Discussion started: 14 September 2026

4.2 Process Chain: From Potential CH_4 Production via Sediment-water Fluxes to the Accumulation of Dissolved CH_4

Potential CH_4 production was significantly correlated with sediment-water CH_4 fluxes, which in turn were significantly correlated with dissolved CH_4 concentrations. Assuming that the potential CH_4 production rates measured under anoxic conditions reflect relative differences in CH_4 production among sediments, the first relationship is consistent with sedimentary CH_4 production contributing to sediment-water CH_4 fluxes. The second relationship is consistent with these fluxes contributing to the accumulation of dissolved CH_4 in the littoral water. Together, these findings are consistent with hypothesis (i) of a process chain from CH_4 production in littoral sediments, via sediment-water CH_4 fluxes, to dissolved CH_4 in the littoral water. However, because all three variables responded strongly to temperature, the observed relationships may partly reflect their shared temperature dependence and therefore do not, by themselves, demonstrate causal propagation along the process chain. Nevertheless, the variables were measured independently, and their covariation is consistent with the proposed mechanism.

An increase in CH_4 production raises pore-water CH_4 concentrations and thereby enhances the concentration gradient towards the sediment-water interface, resulting in a larger sediment-water CH_4 flux (D'Ambrosio and Harrison, 2022). Because this flux acts as a source of dissolved CH_4, larger sediment-water fluxes can be expected to increase dissolved CH_4 concentrations (Peeters et al., 2019). However, the amount of dissolved CH_4 in the water column depends not only on sedimentary inputs, but also on losses through CH_4 oxidation, emission to the atmosphere, and lateral transport or dilution (Bastviken et al., 2008; Encinas Fernández et al., 2016). Thus, changes in sedimentary CH_4 production and sediment-water CH_4 fluxes may be reflected in dissolved CH_4 concentrations, although the strength of this relationship may be modified by transport and loss processes in the sediment and water column.

4.3 Temperature Dependence of Potential CH_4 Production, Sediment-water CH_4 Fluxes, and Dissolved CH_4

Potential CH_4 production increased substantially with temperature (Fig. 2i–k). The Arrhenius model yielded an activation energy of 0.81 eV, corresponding to an approximately 3.3-fold increase in potential CH_4 production between 10 and 20 °C. A similarly strong temperature dependence of methanogenesis has been reported in laboratory and field studies (Lavergne et al., 2021; Schulz et al., 1997).

Sediment-water CH_4 fluxes and dissolved CH_4 concentrations also increased strongly with temperature, with apparent activation energies of 0.94 and 1.11 eV, respectively. These values correspond to approximate increases of 3.8- and 4.9-fold between 10 and 20 °C. Strong temperature dependencies of CH_4 emissions have also been reported in numerous aquatic systems (Yvon-Durocher et al., 2014; Sepulveda-Jauregui et al., 2018).

The apparent activation energies of potential CH_4 production, sediment-water CH_4 fluxes, and dissolved CH_4 concentrations did not differ significantly from one another. This result is consistent with the temperature dependence of sedimentary CH_4 production being propagated through sediment-water fluxes to dissolved CH_4 concentrations in the littoral water. However, given the uncertainty of the estimates and the partly different temperature ranges covered by the experimental production measurements and field observations, small differences in temperature dependence cannot be excluded. Thus, the available

https://doi.org/10.5194/egusphere-2026-5425
Preprint. Discussion started: 14 September 2026

data do not allow us to determine whether diffusion, oxidation, atmospheric exchange, or lateral transport modified the temperature response along the process chain.

4.4 Spatial Differences Along the CH_4 Process Chain

Potential CH_4 production showed a positive relationship with sediment organic carbon content (Fig. 5), suggesting that spatial differences in organic carbon may have contributed to differences in methanogenic potential among sites. However, this relationship was based on only seven site-level observations, and the positive slope was not significantly different from zero ($p = 0.118$; Table S5). Potential CH_4 production was also positively correlated with sediment-water CH_4 fluxes, which were in turn correlated with dissolved CH_4 concentrations. Together, these relationships suggest that spatial differences originating in the sediment may be propagated along the process chain from CH_4 production through sediment-water fluxes to dissolved CH_4 concentrations.

Within LLC, potential CH_4 production did not differ significantly among sites. Sediment-water CH_4 fluxes and dissolved CH_4 concentrations also showed no significant differences among G1, G2, and G3. Thus, the three LLC sites showed relatively homogeneous patterns along the process chain. Within ULC, by contrast, potential CH_4 production was substantially higher at SIP and MUN than at OBG and LBM. A similar spatial pattern was observed in sediment-water CH_4 fluxes, suggesting that spatial differences in sedimentary production were propagated to the flux across the sediment-water interface. However, dissolved CH_4 concentrations did not differ significantly among the four ULC sites. Thus, the pronounced site-level differences in production and sediment-water fluxes were not maintained in the dissolved CH_4 pool. Methane oxidation may have attenuated these differences by removing part of the dissolved CH_4, while lateral mixing may have redistributed CH_4 among littoral and offshore waters (Lofton et al., 2014; Hofmann, 2013; Encinas Fernández et al., 2016). However, the contributions of these processes were not quantified in this study.

Between the two lakes, dissolved CH_4 concentrations were significantly higher in LLC than in ULC, whereas potential CH_4 production and sediment-water CH_4 fluxes did not differ significantly. Lateral mixing may also have contributed to the lake-scale difference in dissolved CH_4 concentrations. Pelagic CH_4 concentrations are typically lower than littoral concentrations, and littoral-pelagic exchange can therefore dilute CH_4-rich littoral water (Encinas Fernández et al., 2016). Because ULC is larger and more exposed than LLC (Fig. 1), its greater fetch and spatial scale may promote stronger horizontal mixing and littoral-pelagic exchange (Okubo, 1971; Peeters and Hofmann, 2015). This could contribute to the lower littoral CH_4 concentrations observed in ULC compared with the smaller and more sheltered LLC. Nevertheless, lateral exchange was not measured directly, and this explanation remains a hypothesis.

https://doi.org/10.5194/egusphere-2026-5425
Preprint. Discussion started: 14 September 2026

5 Conclusions

In summary, our results are consistent with the hypothesis of a process chain from CH_4 production in littoral sediments, via sediment-water CH_4 fluxes, to the accumulation of dissolved CH_4 in littoral water. The similar apparent temperature dependencies of the three variables are consistent with a temperature response along this process chain, although their shared dependence on temperature prevents attributing the observed relationships solely to causal propagation. Within ULC, spatial differences in potential CH_4 production were reflected in sediment-water fluxes but were attenuated in dissolved CH_4 concentrations. Methane oxidation and lateral mixing may have contributed to this attenuation, although their effects were not quantified. Thus, spatial patterns of dissolved CH_4 in littoral waters reflect sedimentary inputs together with transport and transformation processes acting after CH_4 enters the water column.

Code and data availability

The data and analysis code supporting the findings of this study will be deposited in a public repository upon acceptance. During peer review, the data and code are available from the corresponding author upon reasonable request.

Author contribution

KJK and KMC designed this study. KMC acquired the funding for this study. KJK, ASJ and LLR carried out the fieldwork and lab experiments. KJK, ASJ, KMC and FP developed the data analysis. KJK, KMC and FP wrote the original draft of the manuscript. All authors helped to revise the submitted version of the paper.

Competing interests

The authors declare that they have no conflict of interest.

Acknowledgements

We thank Beatrix Rosenberg, Lisa Klingele, Anton Pranger, Devin Jachtmann, Clara Weber, Nico Ströble, and Lena Schwichtenberg for their assistance during field campaigns and laboratory methods. During manuscript preparation, the authors used ChatGPT (OpenAI) to improve language and clarity. All scientific analyses, interpretations, references, and final wording were reviewed and approved by the authors.

https://doi.org/10.5194/egusphere-2026-5425
Preprint. Discussion started: 14 September 2026

Financial support

This work was funded by the German Research Foundation through the LiMeth project (MA 10141/2-1; project number 517753859) and Major Research Instrumentation Grant (INST 38/631-1; project number 516693059).

References

Bastviken, D. (2009). Methane. In G. E. Likens (Ed.), Encyclopedia of Inland Waters (pp. 783-805). Academic Press. https://doi.org/10.1016/B978-012370626-3.00117-4

Bastviken, D., & Johnson, M. S. (2025). Future methane emissions from lakes and reservoirs. Nature Water. https://doi.org/10.1038/s44221-025-00532-6

Bastviken, D., Cole, J. J., Pace, M. L., & Van de Bogert, M. C. (2008). Fates of methane from different lake habitats: Connecting whole-lake budgets and CH4 emissions. Journal of Geophysical Research: Biogeosciences, 113, G02024. https://doi.org/10.1029/2007JG000608

Bertolet, B. L., Koepfli, C., & Jones, S. E. (2022). Lake Sediment Methane Responses to Organic Matter are Related to Microbial Community Composition in Experimental Microcosms. Frontiers in Environmental Science, 10. https://doi.org/10.3389/fenvs.2022.834829

Bodmer, P., Vroom, R. J. E., Stepina, T., del Giorgio, P. A., & Kosten, S. (2024). Methane dynamics in vegetated habitats in inland waters: quantification, regulation, and global significance. Frontiers in Water, 5. https://doi.org/10.3389/frwa.2023.1332968

Bossé, M., Marland, E., Rhoads, G., Sanqui, J. A., & BeMent, Z. (2023). Generalizing R^2 for Deming regressions. Communications in Statistics—Theory and Methods, 52(21), 7731–7743. https://doi.org/10.1080/03610926.2022.2059678

Brandily, C., LeCuff, N., Donval, J.-P., Guyader, V., De Prunele, A., Cathalot, C., Croguennec, C., Caprais, J.-C., & Ruffine, L. (2021). A GC-SSIM-CRDS system: Coupling a gas chromatograph with a Cavity Ring-Down Spectrometer for onboard Twofold analysis of molecular and isotopic compositions of natural gases during ocean-going research expeditions. Analytica Chimica Acta, 1184, 339040. https://doi.org/10.1016/j.aca.2021.339040

Casper, P., Furtado, A. L. S., & Adams, D. D. (2003). Biogeochemistry and diffuse fluxes of greenhouse gases (methane and carbon dioxide) and dinitrogen from the sediments of oligotrophic Lake Stechlin, northern Germany. In R. Koschel & D. D. Adams (Eds.), Lake Stechlin: An approach to understand an oligotrophic lowland lake. Archiv für Hydrobiologie, Special Issues Advances in Limnology, 58, 53–71.

Coleman, D. D., Risatti, J. B., & Schoell, M. (1981). Fractionation of carbon and hydrogen isotopes by methane-oxidizing bacteria. *Geochimica et Cosmochimica Acta, 45*(7), 1033–1037. https://doi.org/10.1016/0016-7037(81)90129-0

Conrad, R. (2005). Quantification of methanogenic pathways using stable carbon isotopic signatures: a review and a proposal. Organic Geochemistry, 36(5), 739-752. https://doi.org/10.1016/j.orggeochem.2004.09.006

D'Ambrosio, S. L., & Harrison, J. A. (2022). Measuring CH_4 fluxes from lake and reservoir sediments: Methodologies and needs. *Frontiers in Environmental Science, 10*, 850070. https://doi.org/10.3389/fenvs.2022.850070

DelSontro, T., del Giorgio, P. A., & Prairie, Y. T. (2018). No Longer a Paradox: The Interaction Between Physical Transport and Biological Processes Explains the Spatial Distribution of Surface Water Methane Within and Across Lakes. Ecosystems, 21(6), 1073-1087. https://doi.org/10.1007/s10021-017-0205-1

https://doi.org/10.5194/egusphere-2026-5425
Preprint. Discussion started: 14 September 2026

Deutscher Wetterdienst (DWD). (2024). HOSTRADA—High-resolution grids of hourly variables for Germany (Version 1.0) [Data set]. Climate Data Center. https://opendata.dwd.de/climate_environment/CDC/grids_germany/hourly/hostrada/

Duc, N. T., Crill, P., & Bastviken, D. (2010). Implications of temperature and sediment characteristics on methane formation and oxidation in lake sediments. Biogeochemistry, 100, 185–196. https://doi.org/10.1007/s10533-010-9415-8

Encinas Fernández, J., Peeters, F., & Hofmann, H. (2016). On the methane paradox: Transport from shallow water zones rather than in situ methanogenesis is the major source of CH4 in the open surface water of lakes. Journal of Geophysical Research: Biogeosciences, 121(10), 2717-2726. https://doi.org/10.1002/2016JG003586

Hilt, S., Grossart, H.-P., McGinnis, D. F., & Keppler, F. (2022). Potential role of submerged macrophytes for oxic methane production in aquatic ecosystems. Limnology and Oceanography, 67(S2), S76–S88. https://doi.org/10.1002/lno.12095

Hofmann, H. (2013). Spatiotemporal distribution patterns of dissolved methane in lakes: How accurate are the current estimations of the diffusive flux path? Geophysical Research Letters, 40(11), 2779-2784. https://doi.org/10.1002/grl.50453

Hofmann, H., Federwisch, L., & Peeters, F. (2010). Wave-induced release of methane: Littoral zones as source of methane in lakes. Limnology and Oceanography, 55(5), 1990-2000. https://doi.org/10.4319/lo.2010.55.5.1990

Internationale Gewässerschutzkommission für den Bodensee (IGKB). (2022). Limnologischer Zustand des Bodensees (Bericht Nr. 44, ISSN 1011-1271).
https://www.igkb.org/fileadmin/user_upload/Downloads/Publikationen/44_gb44gesamtbericht.pdf

Jansen, J., Woolway, R. I., Kraemer, B. M., Albergel, C., Bastviken, D., Weyhenmeyer, G. A., Marcé, R., Sharma, S., Sobek, S., Tranvik, L. J., Perroud, M., Golub, M., Moore, T. N., Råman Vinnå, L., La Fuente, S., Grant, L., Pierson, D. C., Thiery, W., and Jennings, E.: Global increase in methane production under future warming of lake bottom waters, Glob. Change Biol., 28, 5427–5440, https://doi.org/10.1111/gcb.16298, 2022.

Kang, M., Liu, L., & Grossart, H.-P. (2024). Spatio-temporal variations of methane fluxes in sediments of a deep stratified temperate lake. iScience, 27(4), 109520. https://doi.org/10.1016/j.isci.2024.109520

Khatun, S., Berg, J. S., Jézéquel, D., Moiron, M., Escoffier, N., Schubert, C. J., Bouffard, D., & Perga, M.-E. (2024). Long-range transport of littoral methane explains the metalimnetic methane peak in a large lake. Limnology and Oceanography, 69(9), 2095-2108. https://doi.org/10.1002/lno.12652

Lauerwald, R., Allen, G. H., Deemer, B. R., Liu, S., Maavara, T., Raymond, P., Alcott, L., Bastviken, D., Hastie, A., Holgerson, M. A., Johnson, M. S., Lehner, B., Lin, P., Marzadri, A., Ran, L., Tian, H., Yang, X., Yao, Y., & Regnier, P. (2023). Inland Water Greenhouse Gas Budgets for RECCAP2: 2. Regionalization and Homogenization of Estimates. Global Biogeochemical Cycles, 37(5), e2022GB007658. https://doi.org/10.1029/2022GB007658

Lavergne, C., Aguilar-Muñoz, P., Calle, N., Thalasso, F., Astorga-España, M. S., Sepulveda-Jauregui, A., Martinez-Cruz, K., Gandois, L., Mansilla, A., Chamy, R., Barret, M., & Cabrol, L. (2021). Temperature differently affected methanogenic pathways and microbial communities in sub-Antarctic freshwater ecosystems. Environment International, 154, 106575. https://doi.org/10.1016/j.envint.2021.106575

Lessmann, O. (2018). Measuring the methane flux at the sediment-water interface: A comparison of methods [Unpublished thesis]. University of Konstanz.

Lofton, D. D., Whalen, S. C., & Hershey, A. E. (2014). Effect of temperature on methane dynamics and evaluation of methane oxidation kinetics in shallow Arctic Alaskan lakes. *Hydrobiologia, 721*(1), 209–222. https://doi.org/10.1007/s10750-013-1663-x

Londry, K. L., Dawson, K. G., Grover, H. D., Summons, R. E., & Bradley, A. S. (2008). Stable carbon isotope fractionation between substrates and products of Methanosarcina barkeri. Organic Geochemistry, 39(5), 608-621.
https://doi.org/10.1016/j.orggeochem.2008.03.002

https://doi.org/10.5194/egusphere-2026-5425
Preprint. Discussion started: 14 September 2026

Los Gatos Research. (2015). Ultra-Portable Greenhouse Gas Analyzer user manual. Los Gatos Research.

McGinnis, D. F., Greinert, J., Artemov, Y., Beaubien, S. E., and Wüest, A.: Fate of rising methane bubbles in stratified waters: How much methane reaches the atmosphere?, J. Geophys. Res.-Oceans, 111, C09007, https://doi.org/10.1029/2005JC003183, 2006.

Natchimuthu, S., Sundgren, I., Gålfalk, M., Klemedtsson, L., Crill, P., Danielsson, Å., & Bastviken, D. (2016). Spatio-temporal variability of lake CH4 fluxes and its influence on annual whole lake emission estimates. Limnology and Oceanography, 61(S1), S13-S26. https://doi.org/10.1002/lno.10222

Okubo, A. (1971). Oceanic diffusion diagrams. Deep-Sea Research and Oceanographic Abstracts, 18(8), 789–802. https://doi.org/10.1016/0011-7471(71)90046-5

Peacock, M., Davidson, S. J., Kothawala, D. N., Segersten, J., & Futter, M. N. (2023). Spatial and Seasonal Variations in Dissolved Methane Across a Large Lake. Journal of Geophysical Research: Biogeosciences, 128(8), e2023JG007668. https://doi.org/10.1029/2023JG007668

Peeters, F., & Hofmann, H. (2015). Length-scale dependence of horizontal dispersion in the surface water of lakes. Limnology and Oceanography, 60(6), 1917–1934. https://doi.org/10.1002/lno.10141

Peeters, F., & Hofmann, H. (2021). Oxic methanogenesis is only a minor source of lake-wide diffusive CH4 emissions from lakes. Nature Communications, 12(1), 1206. https://doi.org/10.1038/s41467-021-21215-2

Peeters, F., Encinas Fernandez, J., & Hofmann, H. (2019). Sediment fluxes rather than oxic methanogenesis explain diffusive CH4 emissions from lakes and reservoirs. Scientific Reports, 9(1), 243. https://doi.org/10.1038/s41598-018-36530-w

Saunois, M., Martinez, A., Poulter, B., Zhang, Z., Raymond, P. A., Regnier, P., Canadell, J. G., Jackson, R. B., Patra, P. K., Bousquet, P., Ciais, P., Dlugokencky, E. J., Lan, X., Allen, G. H., Bastviken, D., Beerling, D. J., Belikov, D. A., Blake, D. R., Castaldi, S., …Zhuang, Q. (2025). Global Methane Budget 2000–2020. Earth Syst. Sci. Data, 17(5), 1873-1958. https://doi.org/10.5194/essd-17-1873-2025

Schulz, S., Matsuyama, H., & Conrad, R. (1997). Temperature dependence of methane production from different precursors in a profundal sediment (Lake Constance). FEMS Microbiology Ecology, 22(3), 207-213. https://doi.org/10.1016/S0168-6496(96)00091-8

Sepulveda-Jauregui, A., Hoyos-Santillan, J., Martinez-Cruz, K., Walter Anthony, K. M., Casper, P., Belmonte-Izquierdo, Y., & Thalasso, F. (2018). Eutrophication exacerbates the impact of climate warming on lake methane emission. Science of The Total Environment, 636, 411-419. https://doi.org/10.1016/j.scitotenv.2018.04.283

Thebrath, B., Rothfuss, F., Whiticar, M. J., & Conrad, R. (1993). Methane production in littoral sediment of Lake Constance. FEMS Microbiology Letters, 102(3), 279-289. https://doi.org/10.1016/0378-1097(93)90210-S

Wessels, M., Anselmetti, F. S., Artuso, R., Baran, R., Daut, G., Gaide, S., Geiger, A., Groenveld, J. D., Hilbe, M., Möst, K., Klauser, B., Niemann, S., Roschlaub, R., Steinbacher, F., Wintersteller, P., & Zahn, E. (2015). Bathymetry of Lake Constance—A high-resolution survey in a large, deep lake. zfv—Zeitschrift für Geodäsie, Geoinformation und Landmanagement, 140, 203–210. https://doi.org/10.12902/zfv-0079-2015

Whiticar, M. J. (1999). Carbon and hydrogen isotope systematics of bacterial formation and oxidation of methane. Chemical Geology, 161(1), 291-314. https://doi.org/10.1016/S0009-2541(99)00092-3

Whiticar, M. J., Faber, E., & Schoell, M. (1986). Biogenic methane formation in marine and freshwater environments: CO2 reduction vs. acetate fermentation—Isotope evidence. Geochimica et Cosmochimica Acta, 50(5), 693-709. https://doi.org/10.1016/0016-7037(86)90346-7

https://doi.org/10.5194/egusphere-2026-5425
Preprint. Discussion started: 14 September 2026

Wiesenburg, D. A., & Guinasso, N. L. (1979). Equilibrium solubilities of methane, carbon monoxide, and hydrogen in water and sea water. Journal of chemical and engineering data, 24(4), 356-360. https://doi.org/10.1021/je60083a006

Yvon-Durocher, G., Allen, A. P., Bastviken, D., Conrad, R., Gudasz, C., St-Pierre, A., Thanh-Duc, N., & del Giorgio, P. A. (2014). Methane fluxes show consistent temperature dependence across microbial to ecosystem scales. Nature, 507(7493), 488-491. https://doi.org/10.1038/nature13164